Received 17 November 2021; revised 5 January 2022; accepted 28 January 2022. Date of publication 1 February 2022; date of current version 22 February 2022.
The review of this article was arranged by Editor A. Nathan.

Digital Object Identifier 10.1109/JEDS.2022.3148129

Statistical Study of Degradation of Flexible Poly-Si TFTs Under Dynamic Bending Stress

BIN LI, WENJUAN ZHOU, YANG HU, MENGJUN DU, MINGXIANG WANG (Senior Member, IEEE), DONGLI ZHANG (Member, IEEE), AND HUAISHENG WANG

School of Electronic and Information Engineering, Soochow University, Suzhou 215006, China

CORRESPONDING AUTHOR: M. WANG (e-mail: mingxiang_wang@suda.edu.cn)

This work was supported in part by the National Natural Science Foundation of China under Grant 61974101 and Grant 61971299; in part by the Natural Science Foundation of Jiangsu Province of China under Grant BK20201201; in part by the State Key Laboratory of ASIC and System, Fudan University, under Grant 2021KF005; in part by the Suzhou Science and Technology Bureau under Grant SYG201933; and in part by the Jiangsu Higher Education Institute of China under Grant 19KJB510058.

ABSTRACT Degradation of flexible low-temperature poly-Si thin film transistors (TFTs) under dynamic bending cycles is investigated with statistical method. I_{ON} degradation data of different bending cycles and bending conditions are compared to five different statistical distribution models, and it is determined that the Gamma distribution best fits degradation data. Based on the model, the reliability of TFTs under a given stress condition can be evaluated under two typical application scenarios: (1) reliability prediction for large bending cycles; (2) reliability evaluation based on stress test with limited sample size.

INDEX TERMS Flexible poly-Si TFTs, dynamic bending, degradation, statistical distribution, reliability evaluation.

I. INTRODUCTION

Currently, electronic products become increasingly flexible such as foldable flat panel displays. As the basic driving element of flexible electronic systems, flexible thin-film transistors (TFTs) are subject to various mechanical stresses such as bending and stretch. Mechanical reliability of flexible TFTs becomes a concerned issue, on which a lot of research efforts have been focused. In case of flexible low temperature poly-Si (LTPS) TFTs under bending stresses, the investigation covers TFT degradation and mechanisms [1]–[4], failure analysis [5]–[7], and process or structure optimization [8]–[10]. Nevertheless, for mechanical stress induced degradation in flexible TFTs, there is no statistical analysis reported until now.

Statistical analysis of degradation is essential to evaluate device reliability [11]. For example, in the study of electromigration of deep submicron interconnects, statistical distribution is used for lifetime prediction [12]. In active-matrix displays, each pixel circuit works independently, thus the electrical stress state of each TFT is different. However, under a mechanical stress in either bending or stretch, a large number of TFTs are located within the same stress field and they suffer the same stress. In this case, although degradation or failure of an individual TFT is random in nature, the lifetime or reliability of such a group of devices can be reasonably evaluated with a given failure criterion. However, it requires the statistical distribution model of the degradation data to be determined first [13].

The purpose of this work is to determine the degradation distribution model of flexible LTPS TFTs under dynamic bending stress, through a systematic statistical analysis on their mechanical degradation. It is found that the statistical distribution of I_{ON} degradation follows the Gamma distribution model. Based on the model, the reliability of stressed TFTs can be evaluated in two typical application scenarios.

II. EXPERIMENTS

Fig. 1 shows the cross-sectional diagram of flexible p-channel LTPS TFTs fabricated on the polyimide (PI) substrate. A rigid glass substrate was used as a device holder, on which a 17-μm PI film was coated and baked at a higher temperature for curing. Then, SiN_x and SiO_x multilayers were deposited on the PI substrate by plasma-enhanced chemical

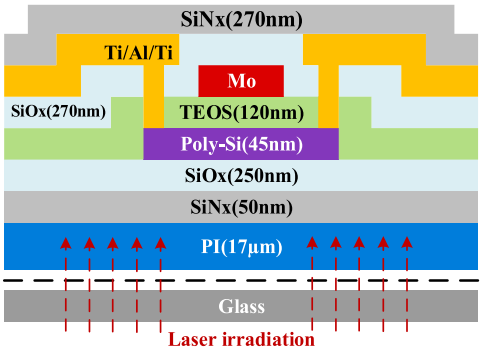

FIGURE 1. Schematic cross section of flexible LTPS TFTs fabricated on PI substrate.

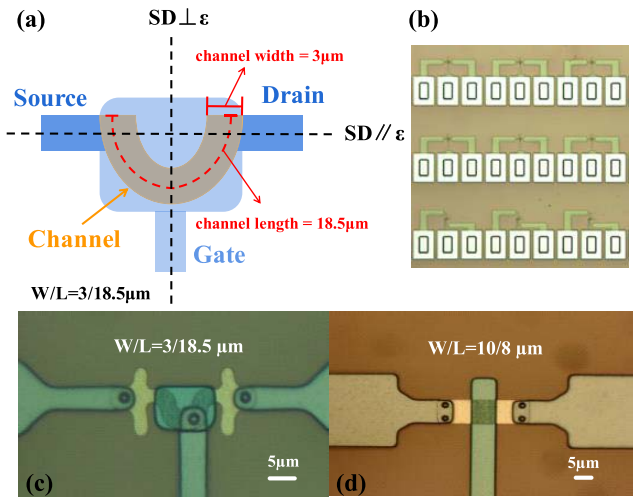

FIGURE 2. (a) Simplified top-view diagram, (b) layout of the TFT matrix, (c) micrograph of a U-shaped channel LTPS TFT, (d) micrograph of a conventional rectangular channel LTPS TFT (SD and ε respectively represent the direction along the source-drain and bending axis).

vapor deposition (PECVD) to block water vapor and oxygen. Subsequently, a 45-nm PECVD a-Si film was deposited and dehydrogenated at 450 °C, followed by excimer laser annealing for crystallization. After active region definition, a 120-nm-thick SiO_2 was deposited as gate insulator (GI). Next, 250-nm Mo alloy was sputtered and patterned as gate electrodes. Boron ions were implanted and activated to form the source and drain regions. A 270-nm-thick SiO_x is deposited as an interlayer dielectric. Subsequently, contact holes were opened and Ti–Al–Ti triple layers metallization was formed, followed by deposition of 270-nm SiN_x passivation layer. Finally, PI film with TFTs whereon was detached from the glass substrate by using laser irradiation. The lift-off process of flexible LTPS TFTs only slightly affects the device characteristics [14].

The structure diagram, layout and micrograph of LTPS TFTs are shown in Fig. 2 (a), (b) and (c). The channel is U-shaped with channel width (W)/length (L) = 3/18.5 μm. Conventional rectangular channel TFTs with W/L = 3/18.5 μm were also used as a control group, as shown in Fig. 2 (d). On the PI substrate, a relatively large sample-sized 84 identical TFTs

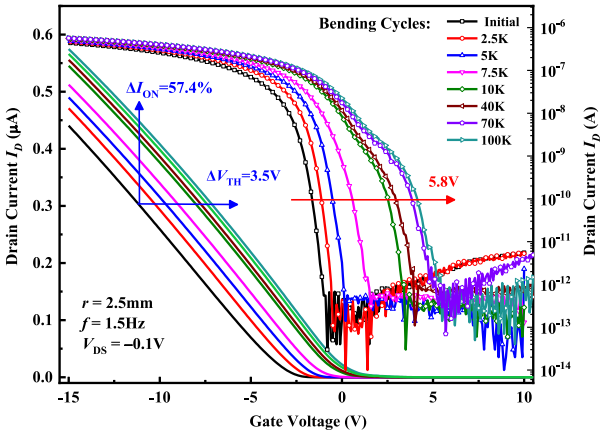

FIGURE 3. Evolution of transfer characteristic curve with dynamic bending cycles.

are subject to dynamic bending stress at the same time. As indicated in Fig. 2 (b), the TFT sample is about 1×2 cm^2, which is cut from the TFT TEG from G6 (1.5×1.85 m^2) production line of Visionox co. ltd. 84 identical TFTs are arranged in three rows, with 28 TFTs in each row. The source-drain direction of the first two rows is parallel to the bending axis (SD∥); while that of the third row is perpendicular to it (SD⊥). The mean and standard deviation of I_{ON} of all TFTs are respectively 2.46×10^{-7} A and 2.14×10^{-8} A. The initial characteristics of these devices have good uniformity. The bending radius (r) includes 2.5, 3.3, and 5 mm, while frequency (f) is 1, 1.5, or 2 Hz. Degradation of electrical characteristics of all TFTs is monitored at 10 preset bending cycles (N) from 10K to 100K. All TFT characteristics are measured by Agilent B1500A semiconductor parameter analyzer in a flat state. The on-state current (I_{ON}) is defined as I_D at $V_G = -12$ V ($V_{DS} = -0.1$ V), the threshold voltage (V_{TH}) is defined as V_G at $I_D = W/L\times10^{-7}$ A ($V_{DS} = -0.1$ V). The percentile change relative to the initial I_{ON} (ΔI_{ON}) is used to characterize the device degradation.

III. RESULTS AND DISCUSSIONS

Typical degradation of flexible LTPS TFTs under dynamic bending stress is shown in Fig. 3. As bending cycles N increases to 100K, V_{TH} shifts along the positive V_G direction by 3.5 V, I_{ON} increases by 57.4%, and the field-effect mobility (μ_{FE}) decreases slightly from 78.6 to 71.0 cm^2/V s. A "hump" is gradually formed with the subthreshold region of the transfer characteristic shifted by +5.8 V. All degradation features are consistent with results reported by previous studies [3], [4]. The positive shift of the transfer characteristic is due to bending stress induced traps in the GI or at the channel/GI interface, and fixed negative charges trapping. V_{TH} degradation of poly-Si TFTs observed in the air ambient is controlled by the synergistic effect of O_2 and H_2O vapor [4]. The "hump" is due to the parasitic transistor effect as clarified in [3].

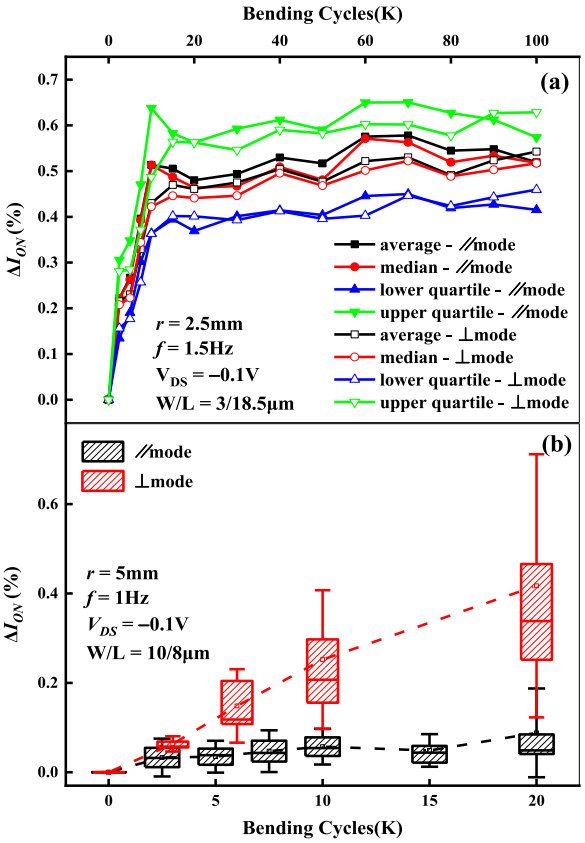

FIGURE 4. Comparison of the degradation of (a) U-shaped channel, and (b) conventional rectangular channel LTPS TFTs under ∥ mode and ⊥ mode.

Previously, it was reported [15] that under static bending the electrical characteristic of U-TFTs is relatively insensitive to the bending direction compared to the conventional rectangular channel TFTs. In the dynamic bending test of this study, the bending is respectively in the ∥ and ⊥ mode for 56 or 28 TFTs. I_{ON} degradation data of all TFTs are collected at 10 preset bending cycles. Fig. 4(a) compares I_{ON} degradation trend with N in the two modes, plotted respectively with the average, median, upper and lower quartile obtained from the 56 or 28 degradation data at a given N. One sees that all curves follow a similar trend, and difference between the degradation of the two modes is very small. For conventional rectangular channel TFTs Fig. 4(b) compares I_{ON} degradation of the two modes using box-plot. In contrast, the I_{ON} degradation of the ⊥ mode is far larger than that of the ∥ mode. It demonstrates that the degradation of the U-channel TFTs is insensitive to the direction of the dynamic bending axis.

Based on statistical hypothesis testing [16], one can go further to quantitatively determine if the degradation is irrelevant to the direction of the bending axis. For each N, two data sets of the ∥ and ⊥ mode respectively includes 56 and 28 degradation data. First do the F-test to check the homogeneity of the variance of the two data sets, and then do the T-test to check the homogeneity of the mean. Normally the

TABLE 1. p-values of hypothesis test for ∥ and ⊥ mode degradation data.

Cycles	10K	20K	30K	40K	50K
F-test	0.3522	0.7223	0.5440	0.5657	0.4737
T-test	0.1836	0.2827	0.1508	0.0593	0.1111
Cycles	**60K**	**70K**	**80K**	**90K**	**100K**
F-test	0.3942	0.3898	0.2926	1.98e-6	0.3180
T-test	0.3800	0.5028	0.2705	0.9072	0.8462
S-Level	α_0=0.05				

statistical confidence level is set as 95%, correspondingly the significance level (S-level) α_0 is 0.05. A p-value of the test larger than α_0 means that the difference between the two sets is not significant. As listed in Table 1, except for the F-test at N = 90K, all other p-values of both tests at different Ns satisfy >0.05, suggesting that there should be no statistical difference in I_{ON} degradation between the two modes, and two sets of degradation data should belong to a single data population. Hence in the following study on the statistical distribution model of the I_{ON} degradation, the two bending modes are no longer distinguished. For each bending cycle, degradation data from all 84 samples are included. To determine the statistical distribution model, the Akaike Information Criterion (AIC) [17], [18] is used. AIC value can measure the goodness of a chosen distribution model fitting the actual degradation data. The smaller the AIC value, the better the goodness of the model. Five statistical distribution models are evaluated: Gamma, Normal, Lognormal, Weibull and Exponential, which are the most commonly used in reliability engineering [19].

Based on a set of degradation data at a given N, AIC value can be calculated with the following equation, assuming that errors between the chosen model and actual data follows an independent Normal distribution [18]:

$$AIC = 2k + nln\left(\frac{SSR}{n}\right) \tag{1}$$

where k is number of model parameters, n is the sample size, SSR is the Sum Square of Residue between the model prediction and actual data, i.e.,

$$SSR = \sum_{i=1}^{n} (T_i - t_i)^2 \tag{2}$$

Here t_i is the ith data of ΔI_{ON}, and T_i the value of the chosen distribution model at quantile corresponding to t_i. To calculate AIC value of the Normal distribution as an example. Assume a set of degradation data under a stress condition follow the Normal distribution, then its distribution parameters are extracted by fitting the degradation data. Then sort the data in ascending order to obtain t_i (i = 1, 2, 3...). Calculate the quantile for each t_i, and corresponding value of Normal distribution at the quantile T_i is also obtained. Hence, SSR and the AIC value of the Normal distribution can be readily calculated.

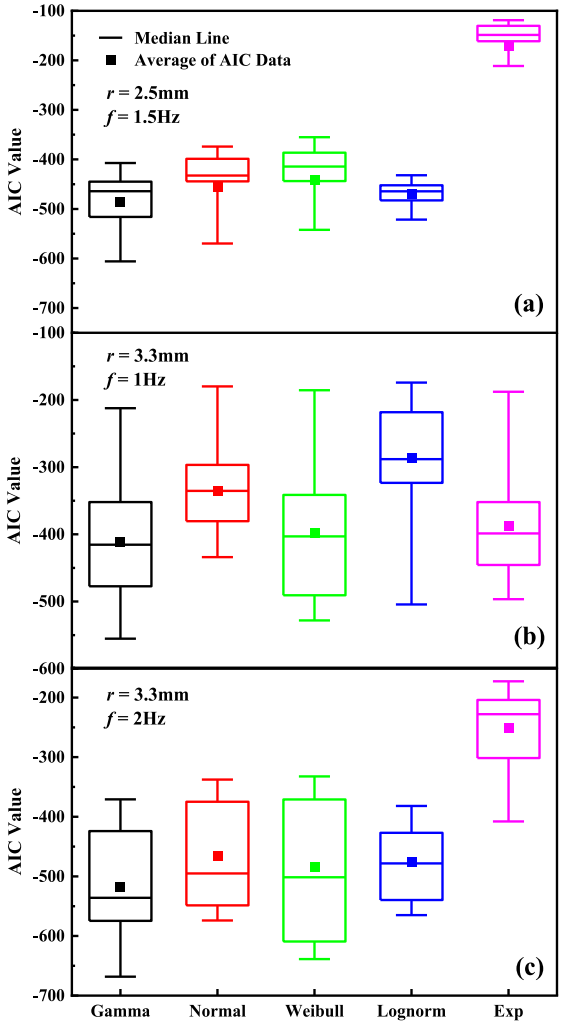

FIGURE 5. AIC box plot of ΔI_{ON} data fitting different distribution models for three stress conditions: (a) r = 2.5mm, f = 1.5Hz; (b) r = 3.3mm, f = 1Hz; (c) r = 3.3mm, f = 2Hz.

Fig. 5 shows box-plot of AIC values of the five distribution models fitting the experimental ΔI_{ON} data respectively under three dynamic bending conditions (a) $r = 2.5$ mm, $f = 1.5$ Hz; (b) $r = 3.3$ mm, $f = 1$ Hz; and (c) $r = 3.3$ mm, $f = 2$ Hz. Each box includes up to 14 AIC values corresponding to degradation data sets at different bending cycles. It clearly shows in Fig. 3 (a)–(c) that the AIC values of the Gamma distribution are smaller than the other four models in terms of the mean, median or the entirety of the box for all three different bending conditions. While the other four distribution models do not show this universality. None of them are even the second-best model for all three bending conditions. Note that device degradations under the three bending conditions are much different, under which the average degradation is respectively 55.8%, 5.32% and 47.0% at $N = 100$K. One can tentatively conclude that the I_{ON} degradation of the p-type flexible LTPS TFTs follows the Gamma distribution model under stress conditions of different bending radius and frequencies.

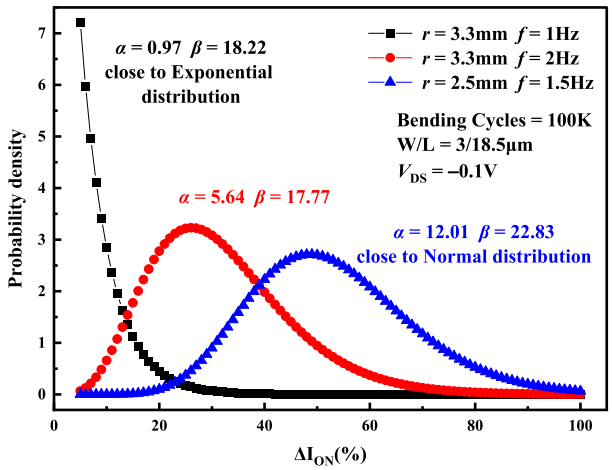

FIGURE 6. Three Gamma distributions for three different stress conditions.

Gamma distribution model is commonly used in statistics [11], [20], and its probability density function (PDF) is as follows:

$$f(\alpha, \beta, x) = \frac{\beta^{\alpha}}{\Gamma(\alpha)} x^{\alpha-1} e^{-\beta x}, x > 0 \tag{3}$$

x is an independent variable, which is ΔI_{ON} in this study. α and β are the shape parameter and scale parameter, respectively. $\Gamma(\alpha)$ is the Gamma function. The mean and variance of the Gamma distribution are:

$$\mu = \frac{\alpha}{\beta}, \sigma^2 = \frac{\alpha}{\beta^2} \tag{4}$$

From Eq. (4), α and β can be also expressed by the mean and variance as:

$$\alpha = \frac{\mu^2}{\sigma^2}, \beta = \frac{\mu}{\sigma^2} \tag{5}$$

The Gamma distribution has some unique features to describe device degradation. First, $x > 0$ means that it is valid for accumulated degradation that always increases with stress time or cycles. Second, the Gamma distribution is positively skewed and has a long tail on the right side, which is in line with most actual degradation phenomena. Third, shape of the Gamma distribution has great flexibility depending on the value of the shape parameter α. As α is close to 1, its PDF is close to an exponential decay; as $\alpha > 20$, it is close to a bell-shaped Normal distribution. Shown in Fig. 6 are the PDF curves of the Gamma distribution under the three different bending conditions. It is close to an exponential distribution for the condition $r = 3.3$mm, $f = 1$Hz; and to the Normal distribution for $r = 2.5$mm, $f = 1.5$Hz. Values of both parameters α and β are given in the figure. Such flexibility allows the Gamma distribution to satisfactorily fit degradation data for very different bending stress conditions and cycles.

Fig. 7(a) and (b) respectively shows extracted Gamma distribution shape and scale parameter α and β dependent on N for three different bending conditions. One sees that α increases linearly with N for all different conditions, while β

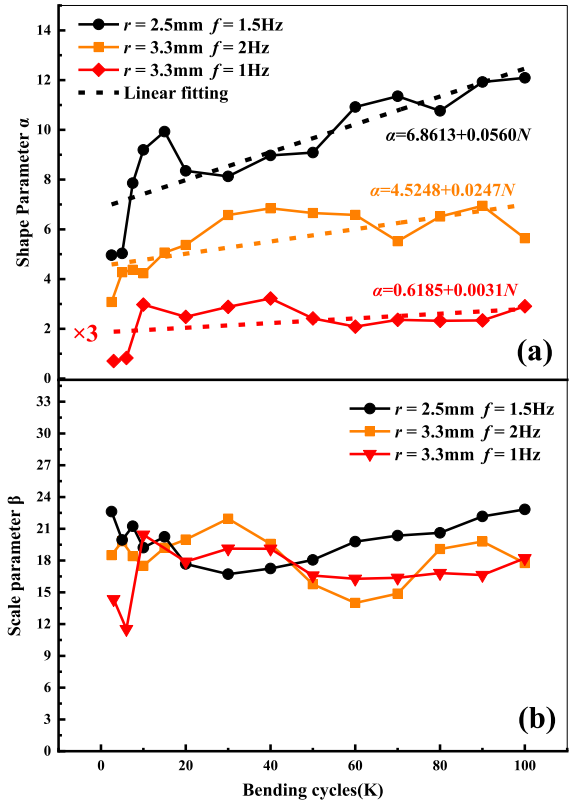

FIGURE 7. Evolution of (a) shape parameter α, and (b) scale parameter β with bending cycles under three different bending conditions.

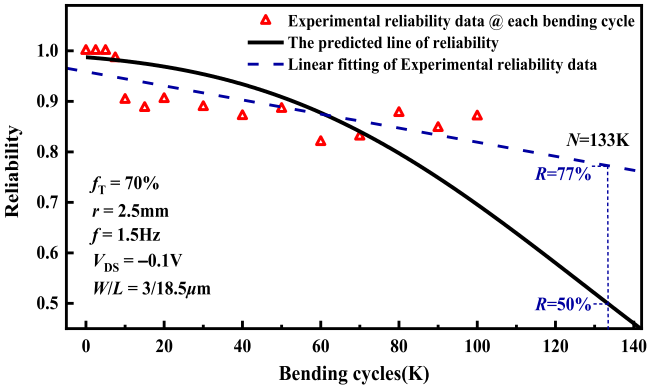

FIGURE 8. Reliability of TFTs depending on N within 140K.

TABLE 2. The reliability evaluation results with r = 2.5mm, 3.3mm, 5mm.

Bending Radius(mm)	2.5	3.3	5
Bending conditions	f=1Hz, N=40K, f_T=50%		
Sample size	6	5	6
Average deg. μ	0.63	0.36	0.31
Variance σ^2	0.36	0.19	0.21
Shape parameter α	1.11	0.67	0.48
Scale parameter β	1.75	1.86	1.52
R	53.4%	75.4%	79.2%

seems has no dependence on N and roughly keeps a constant under different stress conditions. Actually, such dependencies of the two parameters are reasonable. Note that from Eq. (5) the two parameters satisfy $\alpha = \mu\beta$. If β remains basically a constant with N, then α and the mean value of degradation data μ have the same dependence on N. The average amount of degradation μ generally increases linearly with N, consistent with the observed dependency of the shape parameter α. Such simple dependencies of the distribution parameters provide convenience for reliability evaluation using the Gamma distribution.

There are two typical scenarios to evaluate the TFT reliability (R). One is to predict the reliability for large bending cycles with available degradation data of smaller bending cycles. The other is to evaluate TFT reliability of a given stress condition from stress test with only a small sample size.

(1) *Reliability evaluation for large bending cycles:* Under the stress condition $r = 2.5$ mm and $f = 1.5$ Hz, the reliability of TFTs bent to a large cycle number N can be evaluated. Based on existing degradation data, dependency of the shape parameter α on N is obtained as plotted in Fig. 7(a):

$$\alpha = 0.0571N + 6.6923 \tag{6}$$

On the other hand, the scale parameter β is treated as a constant 19.9, which is the average of extracted β values under each bending cycle.

Reliability (R) is the probability of stressed TFTs maintaining their performance until a given cycle. Here, TFT failure threshold (f_T) is defined as $x = \Delta I_{ON} > 70\%$. Thus R as a function of N can be obtained by integrating PDF(x) in the interval $(0, f_T)$:

$$R = \int_0^{0.7} \frac{\beta^\alpha}{\Gamma(\alpha)} x^{\alpha-1} e^{-\beta x} dx \tag{7}$$

Here, α is given by Eq. (6) and $\beta = 19.9$. Fig. 8 shows calculated R as a function of N (the solid line), compared to experimental R values obtained from degradation data statistics at given bending cycles (the triangle symbols). There is a fairly good agreement between the calculated $R(N)$ curve and experimental data. With the increase of N, $R(N)$ constantly decreases. Based on $R(N)$, it is estimated that at $N = 133$K, R will drop to 50%, that is, 50% of the TFTs' I_{ON} degradation is larger than 70%. Note that the prediction is much lower than the intuitively expected value 77% from a linear extrapolation as indicated by the dotted line in the figure.

(2) *Reliability evaluation at given stress conditions:* Since dynamic bending stress induced degradation of flexible LTPS TFTs is demonstrated to follow the Gamma distribution, now R can be reasonably evaluated for any given stress condition based on limited stress tests with a small sample size. For example, stress tests are carried out under three stress conditions: $r = 2.5$, 3.3, or 5 mm and $f = 1$ Hz with only 5-6 TFT samples. The bending cycle is 40K, and f_T is set as 50%. From the stress test, the mean μ and variance σ^2 of the degradation data are obtained first, and parameters of the Gamma distribution α and β are calculated with Eq. (5),

as listed in Table 2. Subsequently, $R(N = 40\text{K})$ can be readily obtained by integrating the Gamma distribution PDF within f_{T} as in Eq. (7). The calculated Rs are listed in Table 2 for each condition, which is seen to increase as r increases.

IV. CONCLUSION

Degradation of p-type flexible LTPS TFTs under dynamic bending stress is studied with statistical method. It is demonstrated that the degradation of U-channel TFTs is not irrelevant to the direction of bending axis. Furthermore, I_{ON} degradation of the flexible LTPS TFTs under dynamic bending stress follows the Gamma distribution. Based on the model, reliability evaluation under two typical application scenarios is carried out: (1) reliability prediction for large bending cycles; (2) reliability evaluation for small sample-sized stress test.

REFERENCES

[1] M. S. Bae, C. Park, D. Shin, S. M. Lee, and I. Yun, "Effects of mechanical stresses on the reliability of low-temperature polycrystalline silicon thin film transistors for foldable displays," *Solid-State Electron.*, vol. 133, pp. 1–5, Jul. 2017, doi: 10.1016/j.sse.2017.04.003.

[2] B.-W. Chen *et al.*, "Effects of repetitive mechanical bending strain on various dimensions of foldable low temperature polysilicon TFTs fabricated on polyimide," *IEEE Electron Device Lett.*, vol. 37, no. 8, pp. 1010–1013, Aug. 2016, doi: 10.1109/LED.2016.2584138.

[3] W. Jiang, B. Li, X. Li, M. Wang, H. Wang, and D. Zhang, "Origin of spontaneous degradation of flexible poly-Si TFTs after dynamic bending," *IEEE Electron Device Lett.*, vol. 41, no. 8, pp. 1205–1208, Aug. 2020, doi: 10.1109/LED.2020.3005526.

[4] M. Du, B. Li, W. Zhou, M. Wang, and D. Zhang, "Origin of degradation of flexible poly-Si TFTs under dynamic bending stress," *IEEE Electron Device Lett.*, vol. 42, no. 11, pp. 1627–1630, Nov. 2021, doi: 10.1109/LED.2021.3116230.

[5] Y. Leterrier *et al.*, "Mechanical failure analysis of thin film transistor devices on steel and polyimide substrates for flexible display applications," *Eng. Fracture Mech.*, vol. 77, no. 4, pp. 660–670, 2010, doi: 10.1016/j.engfracmech.2009.12.016.

[6] K. Hu, S. Cai, L. Lin, X. Gao, and X. Huang, "Failure mechanism of TFT devices on flexible substrate by cyclic bending test," in *Proc. 7th Int. Conf. Comput. Aided Design Thin-Film Transist. Technol. (CAD-TFT)*, Oct. 2016, p. 1, doi: 10.1109/CAD-TFT.2016.7785049.

[7] Z. Sun, M. Wang, S. Xu, and X. Wang, "Instability of flexible low-temperature polycrystalline silicon thin-film transistors under mechanical stresses," in *Proc. IEEE ICSICT*, 2016, pp. 1146–1148, doi: 10.1109/ICSICT.2016.7998676.

[8] S. M. Lee and I. Yun, "Effect of selectively passivated layer on foldable low temperature polycrystalline silicon thin film transistor characteristics under dynamic mechanical stress," *Microelectron. Rel.*, vols. 76–77, pp. 606–609, Sep. 2017, doi: 10.1016/j.microrel.2017.07.092.

[9] W. H. Chen *et al.*, "Stress absorbing LTPS-TFT for highly flexible AMOLED," in *SID Symp. Dig. Tech. Papers*, vol. 48, 2017, pp. 1742–1745, doi: 10.1002/sdtp.12000.

[10] S.-P. Huang *et al.*, "Enhancing repetitive uniaxial mechanical bending endurance at R = 2 mm using an organic trench structure in foldable low temperature poly-si thin-film transistors," *IEEE Electron Device Lett.*, vol. 40, no. 6, pp. 913–916, Jun. 2019, doi: 10.1109/LED.2019.2909966.

[11] A. Birolini, *Reliability Engineering: Theory and Practice*, 4th ed. Heidelberg, Germany: Springer, 2004, pp. 1–26, doi: 10.1007/978-3-662-05409-3.

[12] C. M. Tan, N. Raghavan, and A. Roy, "Application of gamma distribution in electromigration for submicron interconnects," *J. Appl. Phys.*, vol. 102, no. 10, 2007, Art. no. 103703, doi: 10.1063/1.2809449.

[13] H. Y. Wang, X. L. Qi, and Y. W. Wu, "Application of storage life prediction model based on performance degradation distribution in fuze storage life prediction," *AIP Conf. Proc.*, vol. 1890, no. 1, 2017, Art. no. 030001, doi: 10.1063/1.5005189.

[14] Z. Sun, "Degradation behaviors of flexible TFTs under DC gate bias stress," M.S. thesis, School Electron. Inf. Eng., Soochow Univ., Suzhou, China, 2017.

[15] J. Lee *et al.*, "5.8-inch QHD flexible AMOLED display with enhanced bendability of LTPS TFTs," in *J. Soc. Inf. Display*, vol. 26, no. 4, pp. 200–207, 2018, doi: 10.1002/jsid.655.

[16] R. V. Hogg, J. W. McKean, and A. T. Craig, *Introduction to Mathematical Statistics*, 8th ed. Harlow, U.K.: Pearson Educ., 2019, pp. 469–510.

[17] H. Akaike, "A new look at the statistical model identification," *IEEE Trans. Autom. Control*, vol. AC-19, no. 6, pp. 716–723, Dec. 1974, doi: 10.1109/TAC.1974.1100705.

[18] C. K. Minns, J. E. Moore, B. J. Shuter, and N. E. Mandrak, "A preliminary national analysis of some key characteristics of Canadian lakes," *Can. J. Fisheries Aquatic Sci.*, vol. 65, no. 8, pp. 1763–1778, 2008, doi: 10.1139/F08-110.

[19] L. C. Wolstenholme, *Reliability Modelling: A Statistical Approach*, 1st ed. Boca Raton, FL, USA: Routledge, 1999, pp. 21–35, doi: 10.1201/9780203740958.

[20] G. J. Husak, J. Michaelsen, and C. Funk, "Use of the gamma distribution to represent monthly rainfall in Africa for drought monitoring applications," *Int. J. Climatol. J. Royal Meteorol. Soc.*, vol. 27, no. 7, pp. 935–944, 2007, doi: 10.1002/joc.1441.